Journal of Geography and Cartography 2025, 8(2), 11440.
https://doi.org/10.24294/jgc11440

Article

Wheat crop detection by combining NDVI time series, phenology with satellite imagery using machine learning

Samhita Bollepally, Prabhakar Alok Verma*

Indian Institute of Remote Sensing, ISRO, Dehradun 248001, India
*** Corresponding author:** Prabhakar Alok Verma, prabhakar@iirs.gov.in

CITATION

Bollepally S, Verma PA. Wheat crop detection by combining NDVI time series, phenology with satellite imagery using machine learning. Journal of Geography and Cartography. 2025; 8(2): 11440. https://doi.org/10.24294/jgc11440

ARTICLE INFO

Received: 30 January 2025
Accepted: 24 February 2025
Available online: 1 April 2025

Abstract: Creating a crop type map is a dominant yet complicated model to produce. This study aims to determine the best model to identify the wheat crop in the Haridwar district, Uttarakhand, India, by presenting a novel approach using machine learning techniques for time series data derived from the Sentinel-2 satellite spanned from mid-November to April. The proposed methodology combines the Normalized Difference Vegetation Index (NDVI), satellite bands like red, green, blue, and NIR, feature extraction, and classification algorithms to capture crop growth's temporal dynamics effectively. Three models, Random Forest, Convolutional Neural Networks, and Support Vector Machine, were compared to obtain the start of season (SOS). It is validated and evaluated using the performance metrics. Further, Random Forest stood out as the best model statistically and spatially for phenology parameter extraction with the least RMSE value at 19 days. CNN and Random Forest models were used to classify wheat crops by combining SOS, blue, green, red, NIR bands, and NDVI. Random Forest produces a more accurate wheat map with an accuracy of 69% and 0.5 MeanIoU. It was observed that CNN is not able to distinguish between wheat and other crops. The result revealed that incorporating the Sentinel-2 satellite data bearing a high spatial and temporal resolution with supervised machine-learning models and crop phenology metrics can empower the crop type classification process.

Keywords: NDVI; wheat; classification; machine learning; CNN; Random Forest

1. Introduction

Agriculture is one of the most important sectors of the Indian economy, where the majority of the population is dependent on agriculture [1]. Rice, wheat, maize, millet, pulses, and oilseeds are the primary food grains produced in the country. Wherein wheat is one of the staple crops grown in India. Which has significant importance in food security.

Mapping particular crop types is an important component of crop monitoring. Crop type information is required for a variety of decision-making applications like yield estimation, crop insurance, crop rotation, crop damage assessment in case of disaster, etc. [2–5].

The availability of satellite imagery and remote sensing technology has significantly improved crop type mapping [6]. Variety of satellite images are available from low resolution to very high resolution. Suitable imagery can be utilized for crop type mapping depending on the requirement for decision-making. E.g., high spatial resolution is required for crop type mapping for agricultural fields in case of crop insurance [7].

One potential way of classifying the crops on a large scale is by collecting the phenological metrics of the crop [8]. Crop phenology studies the annual sequence of

plant development, which incorporates crop growth and yield formation often driven by climatic conditions. This can be exploited to identify the required crops easily. Remote sensing has become essential for studying crop phenology [9]. Time series data is effective for mapping crop type under the situation that the targeted crop must have a distinguishable growth profile compared to other crops. Wardlow et al. [10] investigated the applicability of time series of vegetation index for identifying crop type. In this study, visually as well as statistically, vegetation index profiles were analyzed. Buermann et al. [11] and Richardson et al. [12] used phenology to understand the impacts of global and regional climate change on the vegetation processes and the vegetation-environment interactions.

The changes in vegetation profile/growth are mainly characterized by phenological metrics like start of the season (SOS), end of the season (EOS), length of the season, and position of peak value. Phenology can be detected using ground-based as well as satellite-based observations. However, ground-based observation can be taken for a few sample sites only, not for each pixel location. Hence, satellite images are a preferred tool to detect pixelwise phenology at different scales [13–15]. Younes et al. [16] derived SOS and the peak of the growing season for mangroves using different sensor imagery using generalized additive models and found that phenology calculated using Landsat and Sentinel-2 is comparable and not from MODIS due to the huge difference in their resolution. Zhu et al. [17] compared 5 phenology extracting methods (piecewise logistic, moving average, local midpoint, polynomial function fitting, and global threshold) to derive phenology from net ecosystem carbon exchange (NEE) data of 72 flux towers in North America to calculate SOS and EOS. In addition, it was observed that the local midpoint method performed better.

Xin et al. [18] evaluated and compared eight phenology retrieving methods (amplitude threshold, the first-order derivative, the second-order derivative, the third-order derivative, the relative change curvature, the curvature change rate, neural networks, and random forests) for calculating SOS and EOS and found machine learning methods outperformed rule-based methods.

Pan et al. [19] showcased the methodology to build NDVI time series from the HJ-1 A/B satellite. They used TIMESAT to extract phenology (SOS, EOS, duration, booting stage). It was found that start/end derived were comparable with local agro-meteorological observations. Gupta et al. [20] used machine learning method to count crop cycles using NDVI time series. Mercier et al. [21] combined Sentinel-1 and Sentinel-2 time series data to derive different phenological stages of wheat and rapeseed crops. Vegetation index data from Sentinel-2, combination of optical and SAR data, MODIS have been used widely for detection and monitoring of crops like rice, wheat, corn [22–26].

Previously, researchers across the world developed algorithms to detect crops using Moderate Resolution Imaging Spectroradiometer (MODIS) due to its high temporal resolution. However, it has very coarse spatial resolution, which makes it less usable for crop type detection, yield estimation, etc., at a larger scale [27–29]. Crop type detection is more difficult in a country like India, where field size is small, staggered, and showing time is highly varying. Nowadays, the availability of Sentinel-2 at 10 m spatial resolution (for optical, NIR) and 5 days temporal

resolution and the availability of Landsat at 30 m spatial resolution make it more useful for detecting crop types more accurately [30,31].

As a crop undergoes different stages of growth, like showing, green-up, heading, and the end of the season. Such stages of crop growth are achieved by different crops at different times from the start of the season. This makes the vegetation index curve useful for discriminating crop types. Some use similarity to the vegetating curve of a specific crop to classify by similarity index and angle parameter. Such methods are dependent on time series. These methods may not work in cases where the characteristics of the crop change in spatial distribution, like a change in SOS for the same crop. Another way of classifying crop type is by extracting phenological characteristics [32,33].

In this research work, we acquired Sentinel-2 images from Google Earth Engine, we developed a method combining phenology, vegetation index profile, and reflectance in R, G, B, and NIR bands to classify wheat crops.

Sentinel-2 is a European satellite containing a multi-spectral instrument (MSI). Sentinel-2 is a passive sun-synchronous orbital satellite at 786 km mean altitude with a wide swath width of 290 km. It is rich in spectral and spatial resolutions, comprising four bands of 10 m resolution, six bands with 20 m resolution, and three bands with 60 m resolution. In addition, it also has a high frequency of revisit time of 10 days near the equator for individual satellites and 5 days by Sentinel-2A and Sentinel-2B together.

2. Study area and dataset

Haridwar district, Uttarakhand, India, covering an area of about 236,000 ha, is chosen as the study area as it is prominently known for its agricultural and horticultural practices. The district's primary land use is agriculture, whereas wheat, rice, and sugar cane are grown chiefly, followed by rangeland, which consists of woodland, shrubland, grasslands, and wetlands. The presence of the river is the primary source for the growth of agriculture. It is also a cause of fertile soil types, ranging from Sandy Loam with high porosity to Loam suitable for horticulture. With the urbanization and development of industries, the urban area’s growth has increased over the past few years, occupying the district's vegetation areas [34].

In addition to satellite data, ground truth points are also required to cross-check the output and to identify the wheat crop fields. Therefore, on-field GPS points are also obtained in the middle of the season. **Figure 1** shows wheat field photograph obtained during filed visit, the crop mask with ground truth points overlaid of Haridwar district, created from ESRI land use map and DEM along with contour lines and major river of the region.

Blue (B02), Green (B03), Red (B04), and Near Infra-Red (B08) bands of the Level-2A product of Sentinel-2 are used. The duration of satellite data is from 15 November 2022 to April 2023. NDVI is calculated using B08 and B04 from Sentinel-2 products. Approximately four hundred data points featuring NDVI values were utilized as input features, while Start of Season (SOS) labels were identified manually.

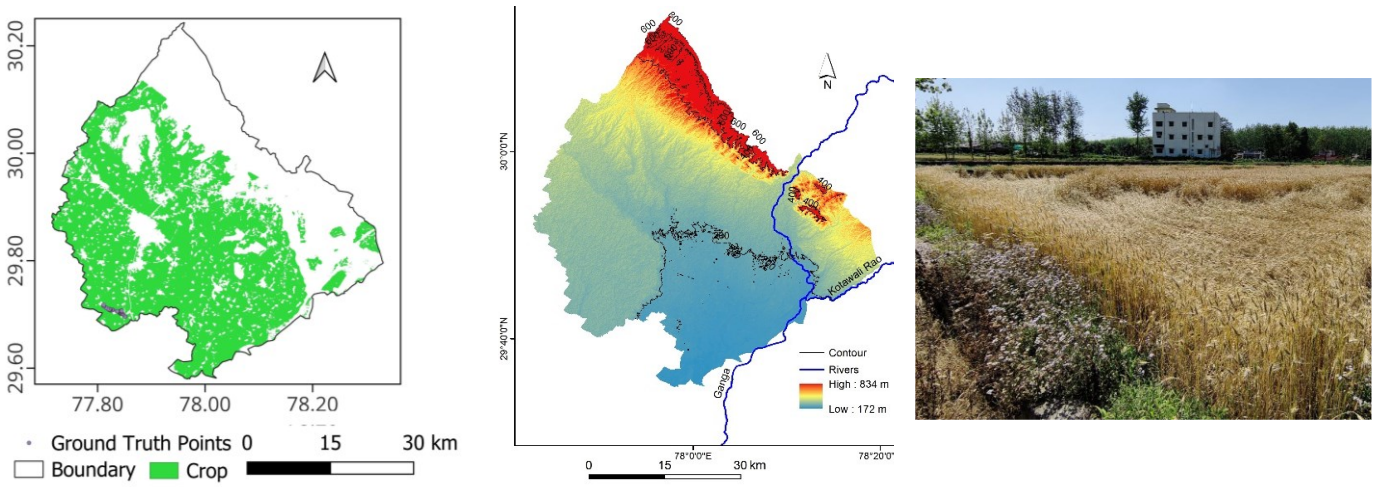

(a) **(b)** **(c)**

Figure 1. (a) Crop mask of study area with ground truth points; **(b)** DEM along with River Ganga; **(c)** field photograph of wheat field captured on 5 April 2023.

3. Methodology

3.1. Data pre-processing

We pre-processed NDVI for each pixel to remove the noise from the time series curve and adopted the Savitzky-Golay filter for this purpose. The Savitzky-Golay filter is a signal-processing filter that fits a polynomial curve for the points in the window to estimate the center of the window and to get a smoothened curve while preserving the shape of the peaks [35]. Window of five observation and polynomial of order 2 was chosen. **Figure 2** shows the vegetation index (VI) profile before and after the SG filter. The overall curvature of both profiles follows a similar trend, but there is a noticeable difference at the beginning, particularly between day 0 and day 20. This discrepancy is likely due to edge effects in the SG filter and seasonal transitions. Around day 40, there is a period with no crop growth, meaning that prior to this, the NDVI should peak and then decline. This expected pattern is better captured in the filtered profile. In contrast, the original curve shows a straight line increment in NDVI from day 0 to day 30, which is unnatural for a crop growth profile. The filtered curve more accurately represents crop growth dynamics by smoothing out sudden peaks and troughs, which are likely caused by errors such as radiometric noise or cloud contamination.

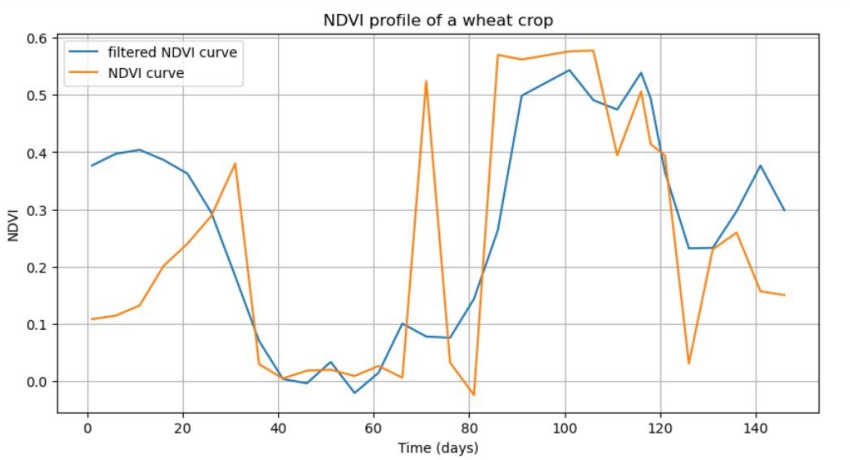

Figure 2. NDVI profile of the wheat crop before and after the SG filter.

3.2. Phenology extraction

We applied three machine-learning algorithms to derive SOS from the NDVI profile. The methods included supervised machine learning models Random Forest, Convolutional Neural Network, and Support Vector Machine [18].

Random Forest uses a number of decision trees and merges their outcomes to reach some conclusion. Random Forest uses the bootstrapping method to randomly sample the data sets and build one decision tree model for each sampled data set. It then creates random feature subsets as the candidate features and selects the best feature combinations to split the internal nodes of decision trees. We built a Random Forest regressor model using the scikit-learn library of Python to extract SOS from the VI profile.

The principle of neural networks is to build a complex network that consists of interacting neurons to make predictions, whereas neurons are basic computing nodes that accept external data or inputs from other neurons and compute outputs. We built a neural network model having a sequence of a layer 1D convolution layer of (32, 5), a 1D Maxpooling layer of (3, 3), a 1D convolution layer of (64, 5), a 1D convolution layer of (128, 5), a 1D Maxpooling layer of (2, 2), flattening, a dense layer, a dropout layer, and a dense layer. Adam optimizer and ReLU activation function were used.

Support vector machine works on the principle of separating two classes using a hyperplane. To extract SOS, an SVM regressor model was built using the scikit-learn library of Python. The RBF kernel was used with degree 3 and epsilon 10.

3.3. Crop type identification

The filtered NDVI values were used as features for the models to extract the season's start. The extracted dates of the start season, filtered NDVI values, and satellite band values were used as features in the classification models. Four hundred random points were generated within the crop mask region, their pixel value in blue, green band, red band, near-infrared band, and NDVI was extracted from time series. Their class labels were identified manually by matching with the ground truth profile. The ground truth data were collected at the field from the Gurkul Narsan block, Haridwar. The GPS coordinates of the ground truth points were collected using the

ODK toolkit. The overall training sample has 242 points from the wheat class and 196 points from other classes.

We considered multivariate input of 6 variables for the classification model. These variables are R, G, B, NIR bands & NDVI, and phenology (SOS). Hence, input consists of a time series of 6 variables of length 23 concatenated together as $(x_1^1, x_2^1, x_3^1 \ldots\ldots, x_{23}^6)$ where x_i^j = denotes the i-th observation of the j-th variable, $i \in [1, 23], j \in [1,6]$.

Two machine learning models (Random Forest, CNN) are used for wheat crop identification. CNN is a neural network framework that can perform classification task over vector, raster data and non-spatial data also. Its architecture includes convoluted, pooling, and fully connected layers that extract features from pixelated inputs through a kernel filter. The convolutional layers apply the filter as a moving window, while the maximum pooling layer downsamples the input vector to reduce computational time. The fully connected layer links the flattened convolutional and pooled layers to the neural network layers for model improvement. The network learns the optimal path to a local minimum using backpropagation and the elementwise applied activation functions, introducing the non-linearity into the network. **Figure 3** shows the architecture of the CNN model used for wheat crop classification.

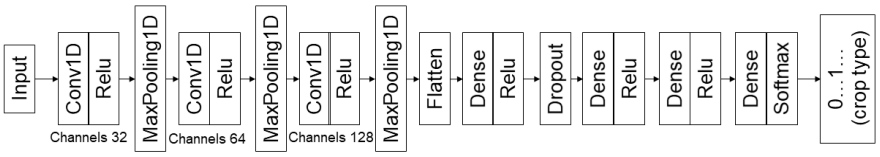

Figure 3. CNN model for classification.

Random Forest, an ensembled supervised algorithm, works on the principle of decision trees. It contains multiple decision trees with various samples from the population data. It chooses the best, based on the vote of predictions, to predict the enhanced accurate outcome irrespective of the scale difference in the features. It measures the weightage of each element on the model's overall accuracy. This depicts the underlying relationship between a certain quality and the target variable. It can also handle the noise and outliers in a large dataset with less training time [36].

4. Result and discussion

The filtered NDVI profile of a pixel having a wheat crop during the winter season is shown in **Figure 4**. The timeline for data under study is 15 November 2022 to April 2023. SOS for wheat crop can be seen around the beginning of January, which is around 50 days from the 15th of November.

The NDVI profile drawn from the satellite time-series data reveals that, on average, the starting day of sowing a wheat crop commenced in end-December. Then again, the predicted results show that the SOS is from January. This may be because the artifacts in the profile, model are not able to capture the exact SOS.

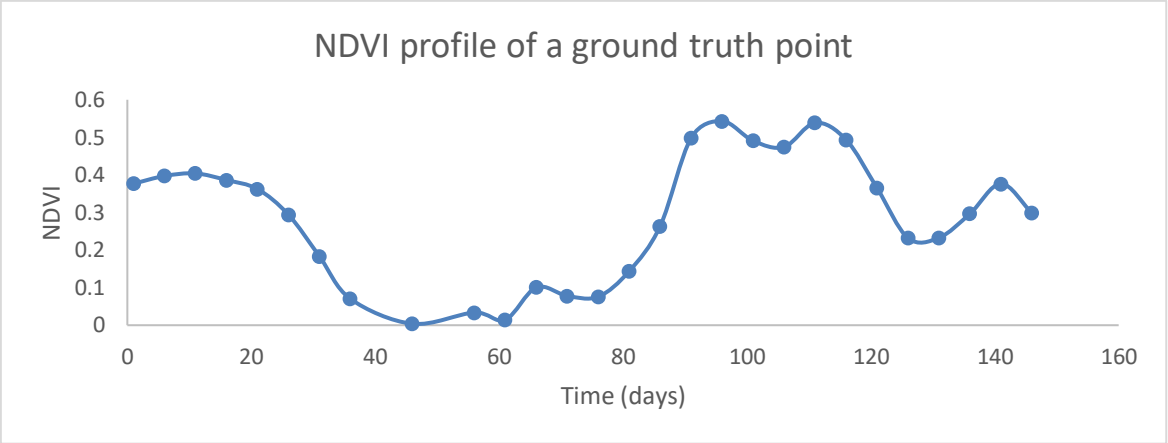

Figure 4. NDVI profile of wheat crop pixel.

A spatial distribution map of satellite-derived SOS for Haridwar district for the winter season is shown in **Figure 5**. All the methods considered have shown slight variation in SOS values. Random Forest gave an outcome of a wide range of dates from January to March. Where most of the southern district has SOS in January, the central part and western part of the district have in the range of January to March, mostly in February month, and at random places of the whole district, it is in March month. SOS calculated by support vector machine is same across the study area, which makes it unreliable. All the fields cannot be expected to have the same SOS. SOS calculated by RF and CNN are quite similar.

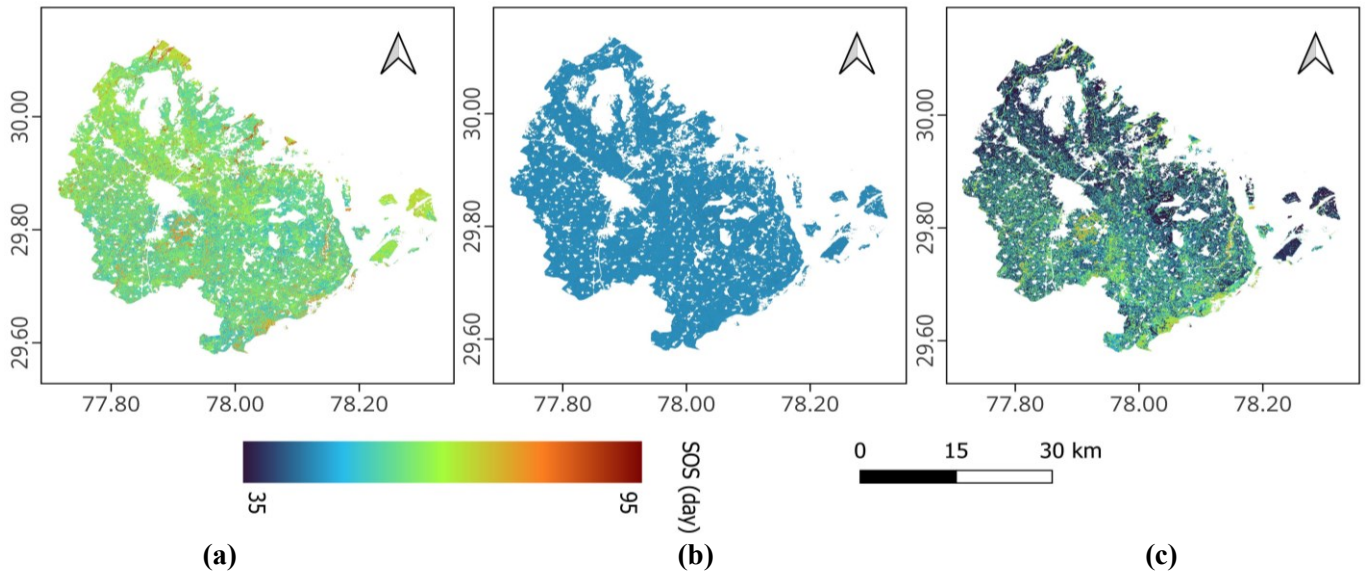

Figure 5. SOS was derived from Sentinel NDVI from 15 November 2022 to April 2023 for the crop mask using **(a)** Random Forest; **(b)** SVM; and **(c)** CNN (day number is counted from the date of the first image, i.e., 15 November).

The performance of machine learning methods for deriving SOS was evaluated using three basic metrics as evaluation indicators, as listed in **Table 1**. Random Forest has an RMSE value of 19.58 days, which is the minimum, followed by the RMSE of CNN & SVM. The correlation coefficient and standard deviation of SVM are zero because, in this case, it seems SVM is unable to learn as it predicts a single

value for all the training samples, which is the 45th day. When the SVM model is applied across the image, it gives the same value of 45 for all the pixels (**Figure 5**). The correlation coefficients between prediction and reference values are 0.15 and 0.65 for Random Forest & CNN, respectively. The standard deviation of Random Forest is 14 days, while CNN has given a standard deviation of 18.5 days. Based on RMSE & standard deviation, Random Forest outperformed SVM and CNN. Hence, for the further process of wheat crop classification, SOS is calculated using Random Forest.

Table 1. Statistical evaluation of SOS derived from satellite based phenology retrieving method and reference data.

Model	RMSE (days)	Correlation coefficient	Standard deviation (days)
Random Forest	19.58	0.15	14
SVM	25.55	0	0
CNN	21.57	0.65	18.5

The wheat crop classification model includes the start of the season of wheat crops derived from the RF model. Wheat crops in Haridwar are usually grown along with mustard and mostly with sugarcane. As the wheat crop reaches its heading stage, sugarcane reaches its maturity stage. Moreover, the initial NDVI values of wheat crops vary with other crops. Hence, SOS can differentiate between wheat and other crops.

A classified map of wheat and non-wheat classes from Random Forest and CNN models is shown in **Figure 6**. The overall spatial distribution of wheat as per the CNN model seems to be overclassified, as the entire crop mask (**Figure 1**) seems to be classified as wheat. Which is not possible as the study region has a significant area under sugarcane cultivation. The wheat map obtained using the Random Forest model seems better compared to CNN, as it is showing a lesser area under wheat cultivation, which leaves the possibility of having other crops in the crop mask (**Figure 1**) region.

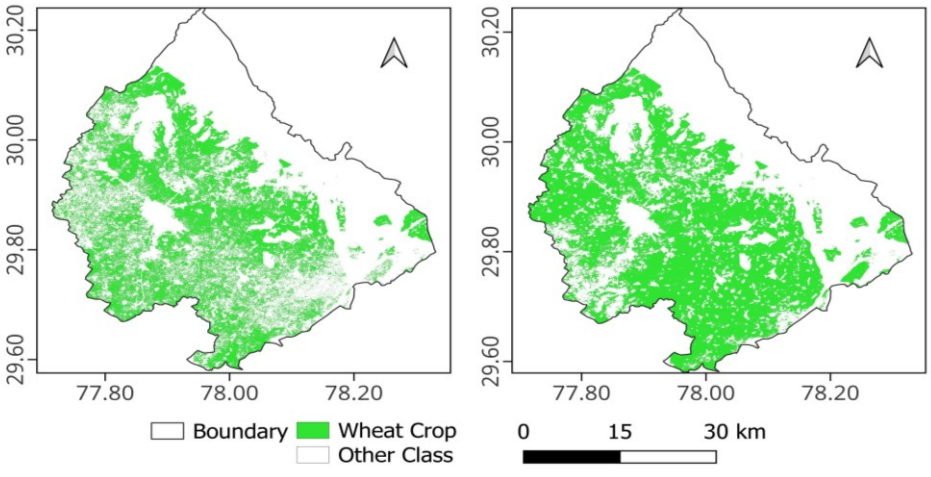

Figure 6. Wheat crop classified map from **(a)** Random Forest; **(b)** CNN.

Table 2 shows the statistical evaluation of CNN and Random Forest classification models to distinguish wheat and non-wheat pixels.

Table 2. Confusion matrix for RF and CNN models.

	Wheat	**Non-wheat**	**User accuracy (%)**	**Wheat**	**Non-wheat**	**User accuracy (%)**
	CNN			**RF**		
Wheat	18	16	52.9	35	15	70
Non-wheat	35	19	35.2	26	56	68.3
Producer accuracy (%)	33.9	54.3	OA: 42 F1-score: 0.43	57.4	78.9	OA: 69 F1-score: 0.73

Random Forest and Convolutional Neural Network models were considered to choose the acceptable model for classifying the wheat crop. These models were made with the start of the season dates, satellite band values (red, blue, green, NIR), and NDVI values. As **Table 2** portrays, the Random Forest model identified the wheat crops as statistically similar to the actual data with an overall accuracy of 69%, hence the suitable model for the wheat crop classification.

The MeanIoU was also calculated as a part of the evaluation. An IoU value of 0.5 was calculated for the Random Forest classification model, implying the model is good. On the other hand, a value of 0.26 was obtained for the CNN classification model. The resulting IoU values infer that the Random Forest model gave better results than the CNN.

5. Discussion

This research provides an analysis of wheat crop classification using Sentinel-2 time-series data combined with phenological parameters, spectral indices, and machine learning algorithms. This study considers the phenological metric Start of Season (SOS) as a critical feature in distinguishing wheat from other crops, especially in regions with diverse cropping patterns and small, fragmented fields, such as Haridwar district in Uttarakhand, India.

The methodology underscores the advantages of using high-resolution satellite imagery Sentinel-2, having a spatial resolution of 10 m and a temporal resolution of five days. This makes it particularly effective for monitoring crops at field level. Pre-processing of the data is done using the Savitzky-Golay filter, which smoothens NDVI time-series data, preserving essential growth characteristics while reducing noise, thereby improving model performance.

The study considers three machine learning algorithms—Random Forest (RF), Convolutional Neural Networks (CNN), and Support Vector Machines (SVM)—to extract SOS and classify wheat crops. Among these, the Random Forest model outperformed the others in terms of accuracy, RMSE, and spatial distribution. The RF model achieved an overall classification accuracy of 69% and a mean IoU of 0.5, surpassing CNN, which showed an overclassified output, and SVM, which failed to provide reliable results. This outcome demonstrates the robustness of ensemble

methods like RF, particularly in scenarios where diverse and high-dimensional datasets are used.

Another strength of the study is its focus on phenological parameters, such as SOS, as a distinguishing feature for wheat. Since sowing dates often vary across farmers in a region, incorporating phenology into classification models offers a more reliable means of differentiating crops. The integration of spectral bands (R, G, B, NIR) and NDVI further enriched the model's inputs, allowing it to account for both spectral and temporal variations.

Overall, this study demonstrates the potential of combining remote sensing data, phenological metrics, and machine learning to address critical agricultural challenges. It offers valuable insights for improving crop monitoring and decision-making processes, particularly in regions where accurate and timely crop type information is essential for food security, yield estimation, and disaster management.

6. Conclusion

In this study, we used Sentinel-2 time-series data to classify the wheat crop in the Haridwar district, Uttarakhand, India, as it has good spatiotemporal properties of 10 m spatial resolution and five days temporal resolution (for combined constellation). Phenological parameter (SOS) was included along with visible, NIR bands and NDVI values to classify wheat crops. Since sowing date is different for farmers so SOS and other phenological parameters can be useful parameter to identify a particular crop. The RMSE value of SOS calculated from the Random Forest model was less than the other models considered. RF gave an RMSE of 19.58 days, and CNN gave an RMSE of 21.57 days. While Support Vector Machine could not learn and gave same SOS for all the pixels. Although CNN gave a better correlation coefficient, Random Forest outperformed it in other metrics as well as in spatial distribution. The Random Forest model identified the wheat crop more accurately with and accuracy of 69% and 0.5 mean IoU. The overall result of this research manifested that the Random Forest model is suitable for both expected outcomes, i.e., for phenology extraction and crop type (wheat) classification. Further following ways may be tried to improve crop type classification accuracy.

- Further study on implementing all the phenology metrics with external parameters like temperature, irrigation, etc., and study on crop characteristics can be conducted.
- The usage of the Red Edge band is also suggested while calculating NDVI, as it highlights the reflectance change and helps in identifying the vegetation with better precision.

Author contributions: Conceptualization, SB and PAV; methodology, SB and PAV; software, SB; validation, SB; formal analysis, SB; investigation, SB; resources, SB; data curation, SB; writing—original draft preparation, SB; writing—review and editing, SB and PAV; visualization, SB; supervision, PAV; project administration, PAV. All authors have read and agreed to the published version of the manuscript.

Data availability: Data used for this research is Sentinel-2 MSI data and data generated for training the model. Sentinel-2 MSI data is freely available at sentinel hub. Data sharing is not possible for training samples.

Institutional review board statement: Not applicable.

Informed consent statement: Not applicable.

Conflict of interest: The authors declare no conflict of interest.

References

1. Pathak H. Impact, adaptation, and mitigation of climate change in Indian agriculture. Environmental Monitoring and Assessment. 2023; 195(1): 52.
2. Kogan F, Kussul N, Adamenko T, et al. Winter wheat yield forecasting in Ukraine based on Earth observation, meteorological data and biophysical models. International Journal of Applied Earth Observation and Geoinformation. 2013; 23: 192–203.
3. Lobell DB, Thau D, Seifert C, et al. A scalable satellite-based crop yield mapper. Remote Sensing of Environment. 2015; 164: 324–333.
4. Meraj G, Kanga S, Ambadkar A, et al. Assessing the yield of wheat using satellite remote sensing-based machine learning algorithms and simulation modeling. Remote Sensing. 2022; 14(13): 3005.
5. Masiza W, Chirima JG, Hamandawana H, et al. A proposed satellite-based crop insurance system for smallholder maize farming. Remote Sensing. 2022; 14(6): 1512.
6. Zhang C, Marzougui A, Sankaran S. High-resolution satellite imagery applications in crop phenotyping: An overview. Computers and Electronics in Agriculture. 2020; 175: 105584.
7. Inglada J, Arias M, Tardy B, et al. Assessment of an operational system for crop type map production using high temporal and spatial resolution satellite optical imagery. Remote Sensing. 2015; 7(9): 12356–12379.
8. Feng S, Zhao J, Liu T, et al. Crop type identification and mapping using machine learning algorithms and sentinel-2 time series data. IEEE Journal of Selected Topics in Applied Earth Observations and Remote Sensing. 2019; 12(9): 3295–3306.
9. Gao F, Zhang X. Mapping crop phenology in near real-time using satellite remote sensing: Challenges and opportunities. Journal of Remote Sensing. 2021; 2: 1–14.
10. Wardlow BD, Egbert SL, Kastens JH. Analysis of time-series MODIS 250 m vegetation index data for crop classification in the US Central Great Plains. Remote sensing of environment. 2007; 108(3): 290–310.
11. Buermann W, Forkel M, O'Sullivan M, et al. Widespread seasonal compensation effects of spring warming on northern plant productivity. Nature. 2018; 562(7725): 110–114.
12. Richardson AD, Hufkens K, Milliman T, et al. Ecosystem warming extends vegetation activity but heightens vulnerability to cold temperatures. Nature. 2018; 560(7718): 368–371.
13. Czernecki B, Nowosad J, Jabłońska K. Machine learning modeling of plant phenology based on coupling satellite and gridded meteorological dataset. International Journal of Biometeorology. 2018; 62: 1297–1309.
14. Pastor-Guzman J, Dash J, Atkinson PM. Remote sensing of mangrove forest phenology and its environmental drivers. Remote sensing of environment. 2018; 205: 71–84.
15. White MA, Nemani RR, Thornton PE, Running SW. Satellite evidence of phenological differences between urbanized and rural areas of the eastern United States deciduous broadleaf forest. Ecosystems. 2002; 5: 260–273.
16. Younes N, Joyce KE, Maier SW. All models of satellite-derived phenology are wrong, but some are useful: A case study from northern Australia. International Journal of Applied Earth Observation and Geoinformation. 2021; 97: 102285.
17. Zhu W, Mou M, Wang L, Jiang N. Evaluation of phenology extracting methods from vegetation index time series. In: Proceedings of the IEEE International Geoscience and Remote Sensing Symposium (IGARSS); 22–27 July 2012; Brussels, Belgium.
18. Xin Q, Li J, Li Z, et al. Evaluations and comparisons of rule-based and machine-learning-based methods to retrieve satellite-based vegetation phenology using MODIS and USA National Phenology Network data. International Journal of Applied Earth Observation and Geoinformation. 2020; 93: 102189.

19. Pan Z, Huang J, Zhou Q, et al. Mapping crop phenology using NDVI time-series derived from HJ-1 A/B data. International Journal of Applied Earth Observation and Geoinformation. 2015; 34: 188–197.
20. Gupta PK, Verma PA, Chauhan, P. Machine Learning Based Crop Cycle Mapping Using Multi Temporal Space Datasets. The International Archives of the Photogrammetry, Remote Sensing and Spatial Information Sciences. 2019; 42: 557–561.
21. Mercier A, Betbeder J, Baudry J, et al. Evaluation of Sentinel-1 & 2 time series for predicting wheat and rapeseed phenological stages. ISPRS Journal of Photogrammetry and Remote Sensing. 2022; 163: 231–256.
22. Mao M, Zhao H, Tang G, Ren J. In-Season Crop Type Detection by Combing Sentinel-1A and Sentinel-2 Imagery Based on the CNN Model. Agronomy. 2023; 13(7): 1723.
23. Xiao X, Boles S, Frolking S, et al. Mapping paddy rice agriculture in South and Southeast Asia using multi-temporal MODIS images. Remote sensing of Environment. 2006; 100(1): 95–113.
24. Chen CF, Son NT, Chang LY, Chen CR. Classification of rice cropping systems by empirical mode decomposition and linear mixture model for time-series MODIS 250 m NDVI data in the Mekong Delta, Vietnam. International Journal of Remote Sensing. 2011; 32(18): 5115–5134.
25. Son NT, Chen CF, Chen CR, et al. A phenology-based classification of time-series MODIS data for rice crop monitoring in Mekong Delta, Vietnam. Remote Sensing. 2013; 6(1): 135–156.
26. Ashourloo D, Nematollahi H, Huete A, et al. A new phenology-based method for mapping wheat and barley using time-series of Sentinel-2 images. Remote Sensing of Environment. 2022; 280: 113206.
27. Franch B, Vermote E, Becker-Reshef I, et al. Improving the timeliness of winter wheat production forecast in the United States of America, Ukraine and China using MODIS data and NCAR Growing Degree Day information. Remote Sensing of Environment. 2015; 161: 131–148.
28. Becker-Reshef I, Vermote E, Lindeman M, Justice C. A generalized regression-based model for forecasting winter wheat yields in Kansas and Ukraine using MODIS data. Remote sensing of environment. 2010; 114(6): 1312–1323.
29. Skakun S, Franch B, Vermote E, et al. Early season large-area winter crop mapping using MODIS NDVI data, growing degree days information and a Gaussian mixture model. Remote Sensing of Environment. 2017; 195: 244–258.
30. Pan L, Xia H. Zhao X, et al. Mapping winter crops using a phenology algorithm, time-series Sentinel-2 and Landsat-7/8 images, and Google Earth Engine. Remote sensing. 2021; 13(13): 2510.
31. Khan A, Hansen MC, Potapov P, et al. Landsat-based wheat mapping in the heterogeneous cropping system of Punjab, Pakistan. International Journal of Remote Sensing. 2016; 37(6): 1391–1410.
32. Li F, Ren J, Wu S, et al. Comparison of regional winter wheat mapping results from different similarity measurement indicators of NDVI time series and their optimized thresholds. Remote Sensing. 2021; 13(6): 1162.
33. Waldner F, Canto GS, Defourny P. Automated annual cropland mapping using knowledge-based temporal features. ISPRS Journal of Photogrammetry and Remote Sensing. 2015; 110: 1–13.
34. Ramadas S, Kuma TK, Singh GP. Wheat production in India: Trends and prospects. In: Recent advances in grain crops research. IntechOpen Publishing; 2019.
35. Cao R, Chen Y, Shen M, et al. A simple method to improve the quality of NDVI time-series data by integrating spatiotemporal information with the Savitzky-Golay filter. Remote Sensing of Environment. 2018; 217: 244–257.
36. Breiman L. Random Forests. Machine learning. 2001; 45: 5–32.